RSC Advances




ROYAL SOCIETY OF CHEMISTRY

www.rsc.org/advances

# Opacity and plasmonic properties of Ag embedded glass based metamaterials

Mohan Chandra Mathpal[*1], Promod Kumar[2], Sachin Kumar[1], Anand Kumar Tripathi[1], Manish Kumar Singh[4], Jai Prakash[3], Arvind Agarwal[1]

[1]*Department of Physics, Motilal Nehru National Institute of Technology, Allahabad-211004, India.*

[2]*Functional nanomaterials research laboratory, department of Physics, National Institute of Technology, Hazratbal, Srinagar-190006, India.*

[3]*Chemical Physics of Materials, Universite Libre de Bruxelles, Campus de la Plaine, CP 243, B-1050, Bruxelles, Belgium.*

[4]*Department of Physics, The LNM Institute of Information Technology, Jaipur-302031, India.*

**Corresponding authors*

Mohan Chandra Mathpal; Email: mohanatnpl@gmail.com.

Tel: +91-532-2271263, Fax: +91-532-2545342.

**Abstract**

Plasmon resonance in noble metals at nanoscale is technologically important for various applications in plasmonic devices. The synthesis and optoelectronic properties of silver based plasmonic metamaterial by ion-exchange ($Ag^+$-$Na^+$) method in soda-lime glass matrix have been investigated. The effects of annealing temperatures on plasmonic resonance of silver nanoclusters are discussed. During annealing the $Ag^+$ are reduced to $Ag^0$ and subsequently form silver nanoparticles in the oxidizing atmosphere. The particle size calculated from Mie theory are in excellent agreement with the size measured from FEGTEM. The prepared materials were characterized by XRD, UV-Vis, RBS, XPS and Raman spectra.

**Keywords:** Optoelectronics; Nanoparticles; Surface Plasmon Resonance; Metamaterials.

## 1. Introduction

Plasmonic nanostructure such as noble metal nanoparticle has attracted many researchers in the past decade due to their intriguing size- and shape-dependent plasmonic and catalytic properties compared to their bulk counterparts which can be used for various applications such as photonics[1], optoelectronics[2,3], biotechnology[4-5] and biomedicine[6]. Metamaterials are made by the combination or stacking of natural materials such as metals, semiconductors, and dielectrics which are structured in such a way that the sizes of their particular pattern and geometries is much smaller than the operating wavelength in order to yield an artificial material with resonance in absorption to electromagnetic excitation. The plasmonic metamaterials based on noble metals such as silver (Ag) and gold (Au) nanoparticles have unusual dispersion and optical properties that arise from localized surface plasmon resonance (LSPR) in nanostructures that access a very large range of wave vectors over a narrow frequency band. Particularly, nanoscale

silver clusters embedded in a transparent dielectric matrix exhibit interesting surface plasmon resonance (SPR) absorption usually observed in the visible region due to their coherent oscillation of conduction band electrons when excited by electromagnetic radiations[7-8]. The plasmonic response of metallic nanoclusters can be tuned by controlling their size, shape, volume, dielectric constant of the matrix and the interparticle separation in the metal nanoparticles which gives a broad spectrum to scientific research in the field of plasmonics[9-10]. Plasmonic materials such as noble metal nanoparticles are considered promising materials for different nonlinear optical processes, like optical limiting[11], optical switching and computing because of their ultrafast nonlinear response[12-16]. Nonlinear optical properties of noble metal nanoparticles dispersed in a transparent dielectric matrix have attracted much attention because of high polarisabilities and fast nonlinear response that can be utilized in making optical devices [17-18]. Ultrafast optical switching devices generally act as key components for the next generation broadband optical networks[17,19]. In general, the major requirements of such devices are plasmonic materials with less linear and nonlinear losses, good optical quality, mechanical stability and ultra-short relaxation time. In this context, silicate glasses containing nanometer sized clusters of noble metals are known to be among the most suitable and promising materials due to their third order non linear susceptibility and ultrafast response[20-21]. Generally high efficient nonlinear optical materials based devices are expected to component for high-capacity communication networks in which the ultrafast switching signal regeneration and high capacity optical recording media is required[20]. Soda-lime silicate glass embedded with silver nanoclusters can be synthesized by various methods such as, ion-implantation, melt-quench techniques, low energy ion- beam mixing, physical vapor deposition, ion exchange methods etc[19-23]. Among these methods the ion exchange method has been considered one of the most important

techniques to introduce metallic nanoclusters inside the glass surface because the technique is simple and does not require any sophisticated equipment. The ion exchange technique combines with thermal annealing has received an increasing attention as it can be used to introduce metallic nanoclusters such as silver, gold and copper into soda-lime matrix[22-25]. The main objective of the work presented in this paper is preparation and study of the plasmonic effects of silver nanoclusters embedded in glass matrix by thermal ion exchange process.

**2. Experimental**

Silver nanoclusters embedded in a soda-lime glass matrix were prepared through the ion-exchange ($Ag^+$-$Na^+$) process followed by thermal annealing in oxidizing atmosphere. Commercial soda lime glass slides (Blue Star Company) with composition (in weight %) of 72.0% $SiO_2$, 14.0% $Na_2O$, 7.1% CaO, 4.0% MgO, 1.9% $Al_2O_3$, 0.6% $K_2O$, 0.3% $SO_3$, 0.1% $Fe_2O_3$) of 0.5 mm thickness were cleaned ultrasonically by using distilled water, trichloroethylene and acetone. Soda lime glass was ion exchanged for few minutes at 370$^{\circ}$C in a molten salt bath having 7 mol% $AgNO_3$ / 93 mol% $NaNO_3$ in a crucible of $Al_2O_3$ .Under these conditions, the silver ions in a molten salt bath diffuse inside the glass matrix and replace the $Na^+$ by $Ag^+$ ions. After inter-diffusion the ion exchange samples were removed from molten bath and cleaned with distilled water and acetone to remove silver nitrate from the surface. The ion-exchanged pristine samples were colorless or were in very faint yellow state. Annealing of these prepared Ag ion exchanged samples were carried out at temperatures 450, 500 and 550°C for 1 h which results in the growth of clusters inside the glass matrix. The exchanged soda-lime glass samples are darkened after annealing significantly, which increases as the annealing temperature increases is shown in Figure 1. The Figure 2 shows the possible exchange and annealing mechanism which takes place during the growth of silver nanoparticles in glass matrix.

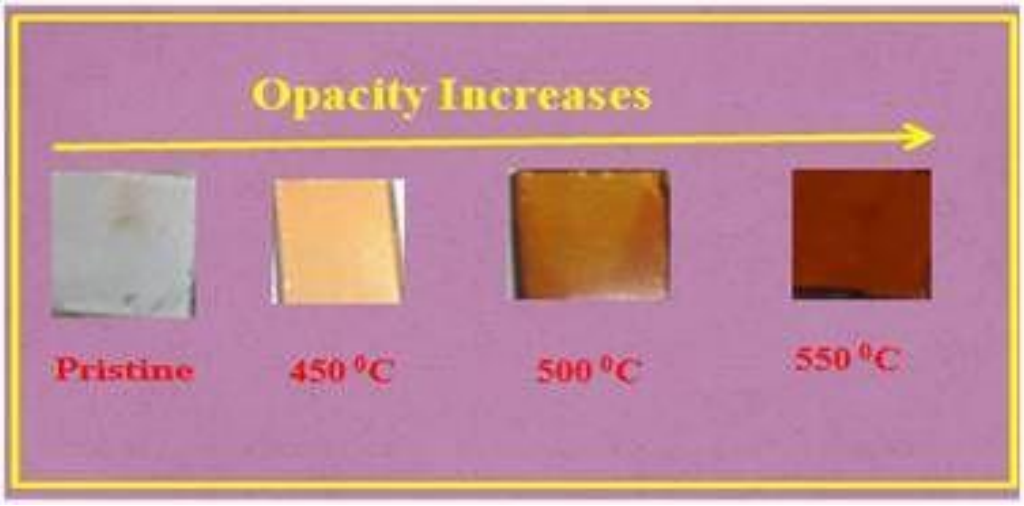


**Figure 1: Opacity increases with increases annealing temperature up to 550°C.**

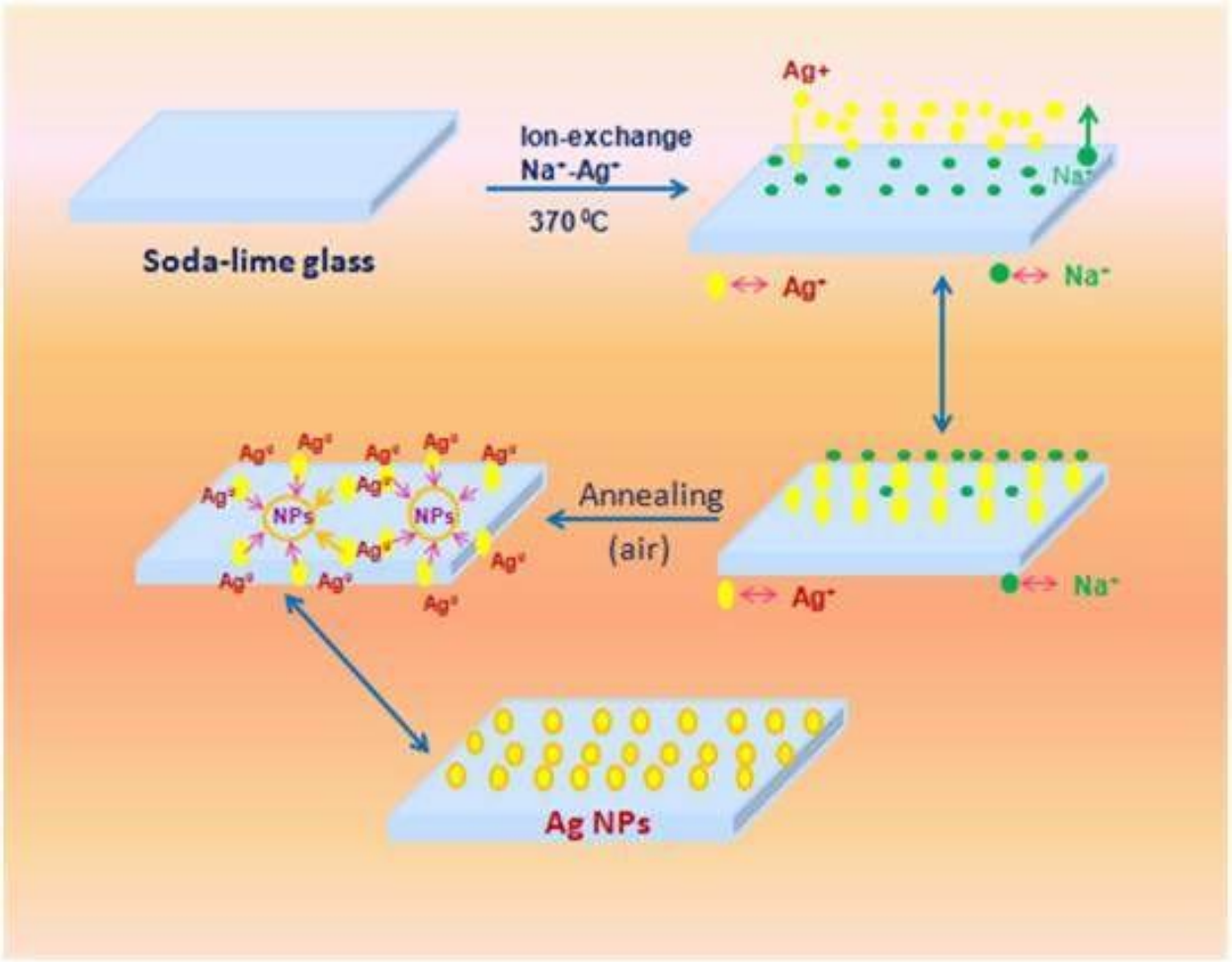


**Figure 2: Exchange and annealing mechanism of silver nanoparticles in soda-lime glass matrix.**

Darkening or increase in the opacity implies that optical absorption has increased consistently with the annealing temperature. The silver nanoclusters formed in commercial soda-lime glass was studied by X-ray diffraction (XRD), UV-visible absorption spectroscopy, field emission gun transmission electron microscope (FEGTEM), Rutherford back scattering (RBS), X-ray photoelectron spectroscopy (XPS) and photoluminescence (PL) measurements to understand the formation mechanism during thermal annealing in air, which is the key to optimize thermal processes for the formation of silver nanoclusters inside the soda-lime glass.

### 3.3. Results and discussion

The XRD pattern and Raman spectra were recorded for the entire samples. The pristine sample and samples annealed at 450°C and 500°C were found to be amorphous in nature, while the sample annealed at 550°C shows face centered cubic (fcc) silver structure (with the plane family {111}, {200}, {220}, and {311}, space group fm3m and JCPDS file no. 4-0787). XRD pattern for the Ag exchanged sample annealed at 550°C is shown in Figure 3.

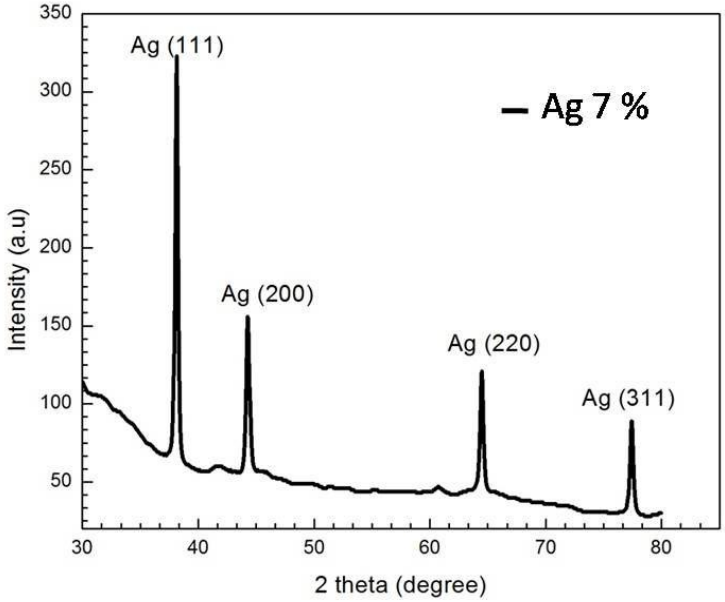


**Figure 3: XRD pattern of Ag exchange sample annealed at 550°C.**

The Raman spectra for ion-exchanged and samples annealed at temperatures 450, 500, and 550°C for 1 hour respectively is shown in Figure 4. The Raman scattering of the pristine sample shown in Figure 4 exhibits similar behavior as it shows for the glass slide (or glass matrices) used in this experiment. There is no Raman band in the observed spectra which is a clear indication that the silver nanoparticles are embedded in glass matrix as metallic silver nanoparticles and does not respond to Raman spectroscopy.

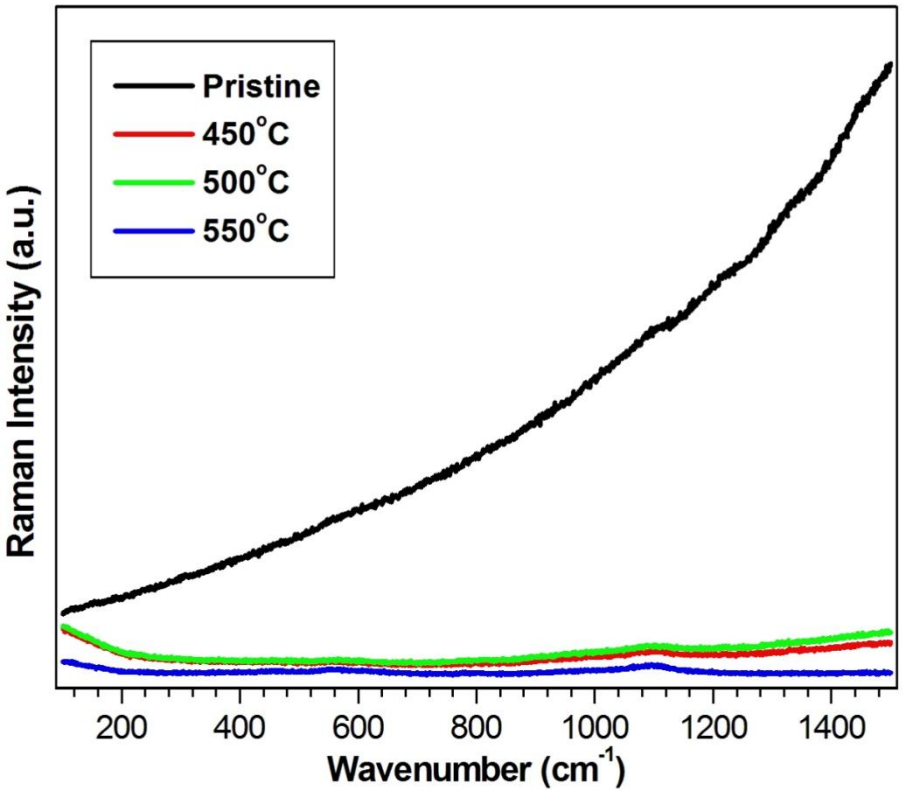


**Figure 4: Raman spectra of pristine and annealed samples at different temperatures.**

Figure 5 show UV-visible absorption spectra of ion-exchanged and thermally treated samples in air at various temperature (450, 500 and 550°C) for 1 hour. The optical absorption spectra of ion-exchanged Ag-doped glass samples do not show any SPR spectra indicating that the silver clusters formation did not occur or the size of Ag nanoclusters were less than 1 nm in size during 2 min ion exchange at 370°C or $Ag^{+}$ ion exists within the pristine sample[23]. After

annealing the silver-exchanged samples at 450°C for 1hr, optical absorption band was observed at 417 nm, which is apparently due to the surface plasmon resonance (SPR) band of silver nanoparticles in the glass matrix. Annealing at higher temperatures (500 and 550°C) resulted in the blue shift of SPR peak. A significant blue shift of 4 nm (from 417 to 413 nm) of the SPR peak was observed in all the annealed samples.

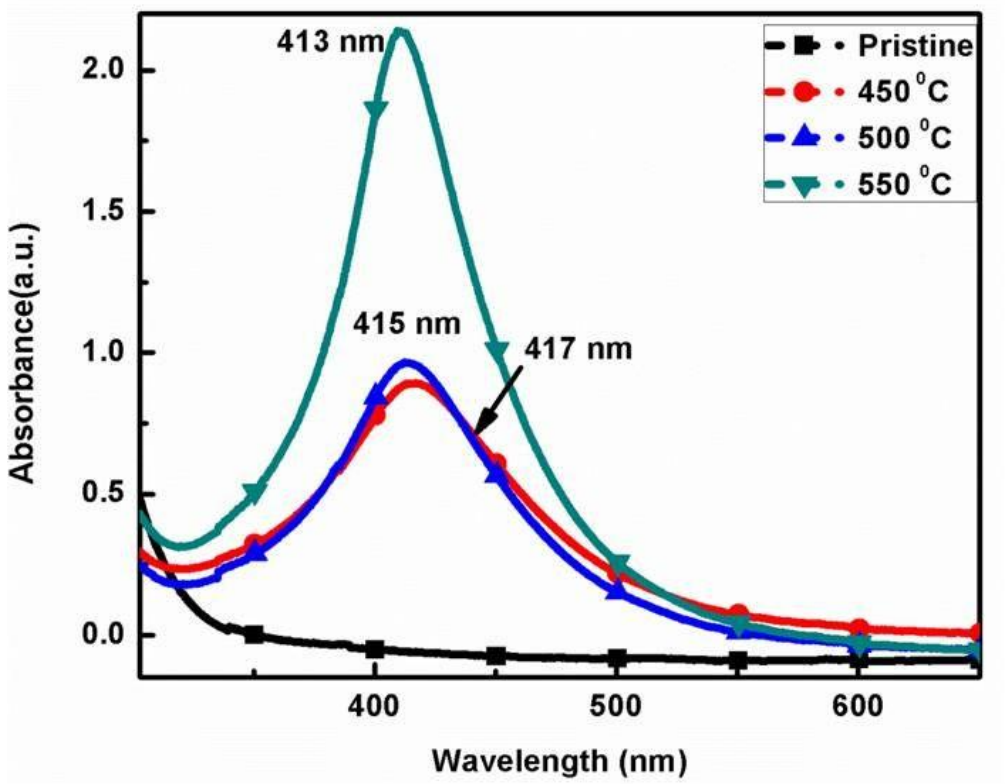


**Figure 5: UV-Vis spectra of Ag ion-exchanged and annealed samples at different temperatures.**

The intensity of the absorption peak increases with the increase of annealing temperature which can be attributed to the thermal growth of the silver nanoclusters in the glass matrix. The shift is attributed to the reduction of the effective refractive index at the interface of the film[24]. The width of the absorption band reduces systematically with the increase in annealing temperature as shown in Figure 6. This is because more $Ag^{+}$ ions were reduced into neutral $Ag^{0}$

atoms indicating an increase of volume fraction of silver nanoclusters in the glass matrix [25]. For a small clusters (R ≤ 10 nm), this kind of decrease in FWHM with increase in clusters size is due to the mean free path effect of electrons as shown in Figure 6[26].

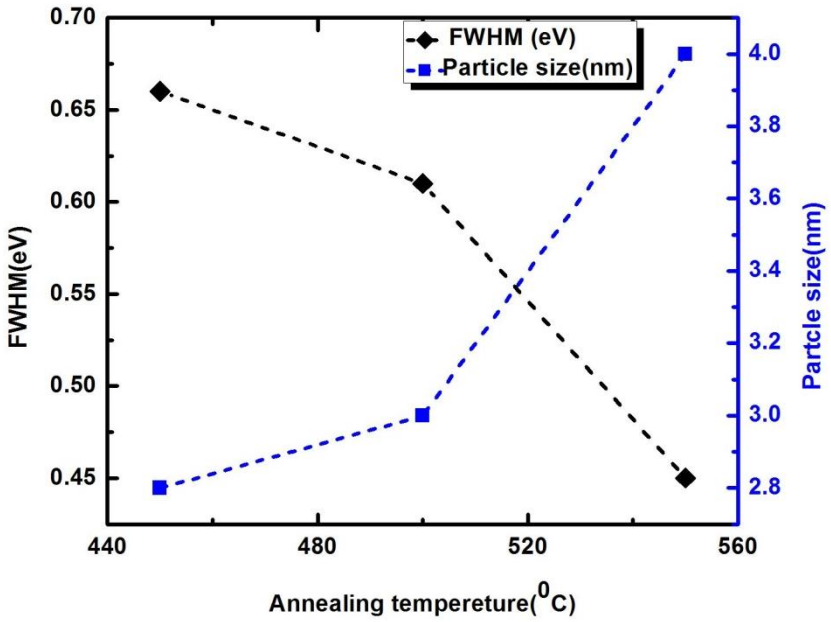


**Figure 6: FWHM and particle size versus annealing temperatures.**

It is well known that the optical properties of Ag nanoclusters dispersed in transparent glass matrix depend on permittivity $\varepsilon(\omega, R)$ of Ag nanoparticles and absorption extinction (K) of Ag nanoparticles, as given in the following in the quasi-static or dipole approximation where $R \ll \lambda$, and $\lambda$ is the wavelength of light[17,27].

$$\varepsilon(\omega, r) = \varepsilon_1(\omega) + i\varepsilon_2(\omega, r) = \varepsilon_1(\omega) + i\left[\varepsilon_{2,\text{bulk}}(\omega) + \eta\frac{\omega_p^2}{\omega^3}\left(\frac{v_F}{r}\right)\right],$$

$$K = \frac{18\pi C\varepsilon_m^{3/2}(\omega)\varepsilon_2(\omega, r)}{\lambda\left((\varepsilon_1(\omega) + 2\varepsilon_m(\omega))^2 + \varepsilon_2^2(\omega, r)\right)}$$

where $\varepsilon_1$ and $\varepsilon_2$ denote the real and imaginary part of the dielectric constant of metal particles respectively, $\varepsilon_m$ is the dielectric constant of the surrounding medium (assumed to be frequency independent), $\omega_p$ is the Drude plasma frequency (for Ag, $\omega_p$= 1.46 × $10^{16}$ $s^{-1}$), $\upsilon_f$ = 1.39 × $10^6$ m/s is the Fermi velocity for bulk silver and C is the volume concentration of the embedded particles; the parameter $\sigma$ is the sum of two additive terms describing size and interface effects. The resonance occurs when $\varepsilon_1(\omega)$= -2 $\varepsilon_m$, i.e. the condition of SPR is fulfilled. The resonance condition is satisfied only for the noble metals such as Ag, Au and Cu nanoparticles at visible wavelengths. Assuming Drude- like the free particles behavior of electrons at nano- sized Ag particles, one can write,

$$R = \upsilon_F \tau$$

Where R is the average radius of the silver nanoclusters and $\tau$ is the mean free time (time between two successive collisions) of the conduction electrons at nano-sized metal particles. Spatial confinement and frequent scattering of conduction electrons over the silver nanoparticles dispersed in a transparent glass matrix leads to quantum fluctuations (ΔE) of the average energy of the free electrons around the surface plasmon resonance. Therefore by applying the Heisenberg's uncertainty principle relation ( $\Delta E.\ \Delta\tau = \hbar$ ), the average cluster diameter is calculated from the full width half maximum of the absorption bands using the formula[28]:

$$d = 2\frac{\hbar \upsilon_F}{\Delta E}$$

where $\hbar$ is the reduced Planck's constant and d is the average diameter of the silver nanoparticles. ΔE (in eV units) is the full width at half maximum of the optical absorption band. The equation is valid as long the size of silver clusters is much smaller than the mean free path of the electrons in the bulk metal[17, 29]. The mean free path of the electrons is about 27 nm at room temperature for bulk silver[30]. By using this equation of Mie theory, the Gaussian profile was

obtained from UV-Vis spectra of Ag nanoparticles and the average size of Ag nanoclusters was calculated to be 2.8, 3.2 and 4.0 nm after annealing in air at 450, 500 and 550°C for 1 hour respectively as shown in Table 1.

**Table 1: Average clusters size estimated by using Mie theory at different annealing temperatures**

| Annealing temperature ($^{o}$C) | Annealing time (h) | SPR wavelength (nm) | FWHM (eV) | Particle size (nm) |
|---|---|---|---|---|
| 450 | 1 | 417 | 0.66 | 2.8 |
| 500 | 1 | 415 | 0.56 | 3.25 |
| 550 | 1 | 413 | 0.45 | 4.0 |

These results show that the size of Ag nanoclusters increases with increase in the annealing temperature due to the diffusion-limited aggregation of silver nanoclusters inside the soda-lime glass[25]. More detailed study on how the dispersion characteristics for the present structure can be affected due to the blue shift and the different amounts of metal losses have been left for further work.

The Figure 7 shows FEGTEM micrographs of annealed sample at 450 and 500°C for 1 hour which was deposited on the carbon coated copper grid. The FEGTEM results clearly show presence of spherical nanoparticles embedded into the glass matrix.

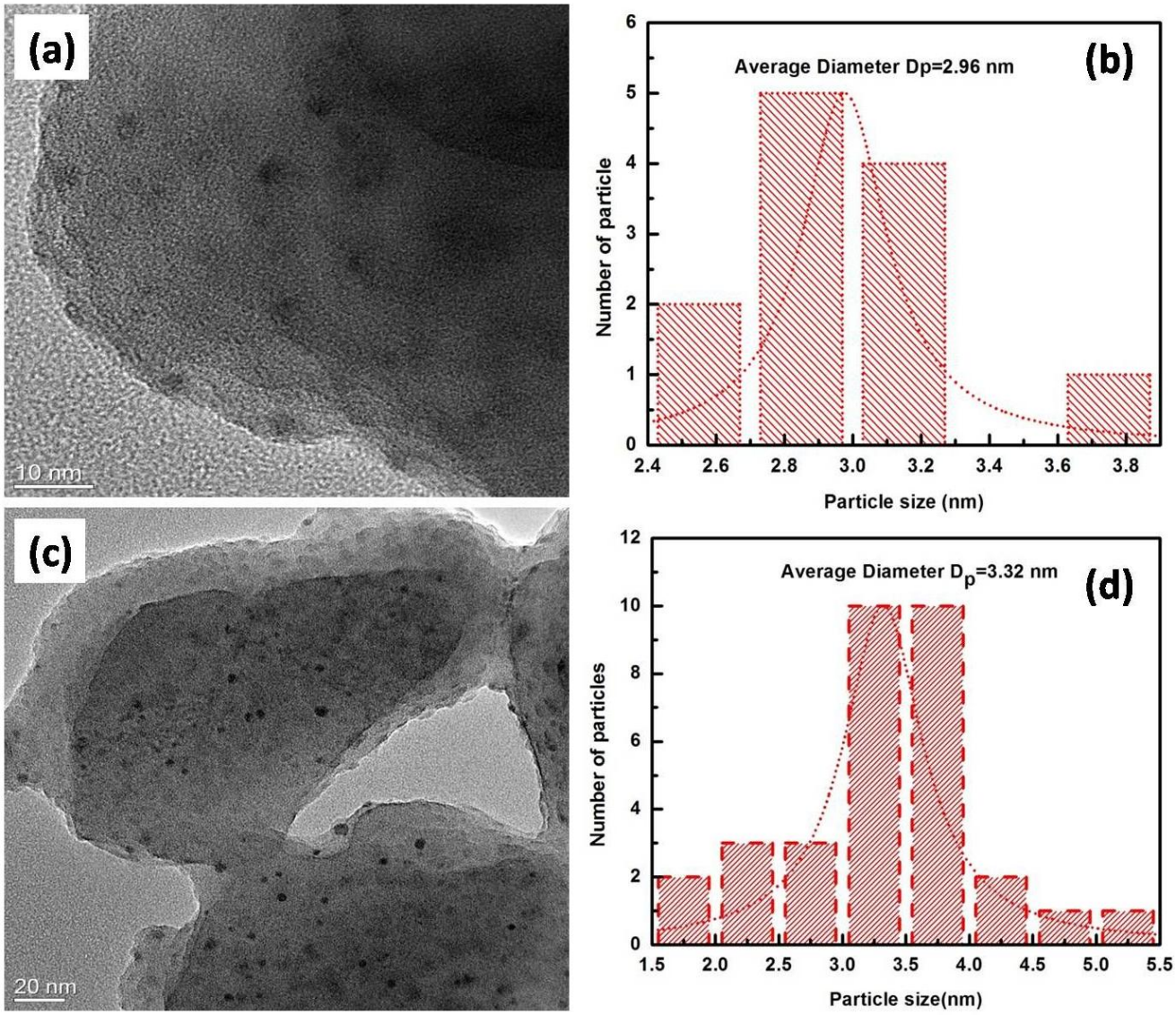


**Figure 7: Silver ion exchanged glass after annealing; (a) FEGTEM image at 450°C for 1h, (b) Average particle size by plotting histogram at 450°C for 1h, (c) FEGTEM image at 500°C for 1h and (d) Average particle size by plotting histogram at 500°C for 1h.**

The Figure 8 shows FEGTEM micrographs of annealed sample at 550°C for 1 hour which was deposited on the carbon coated copper grid. The FEGTEM results clearly show presence of spherical nanoparticles embedded into the glass matrix.

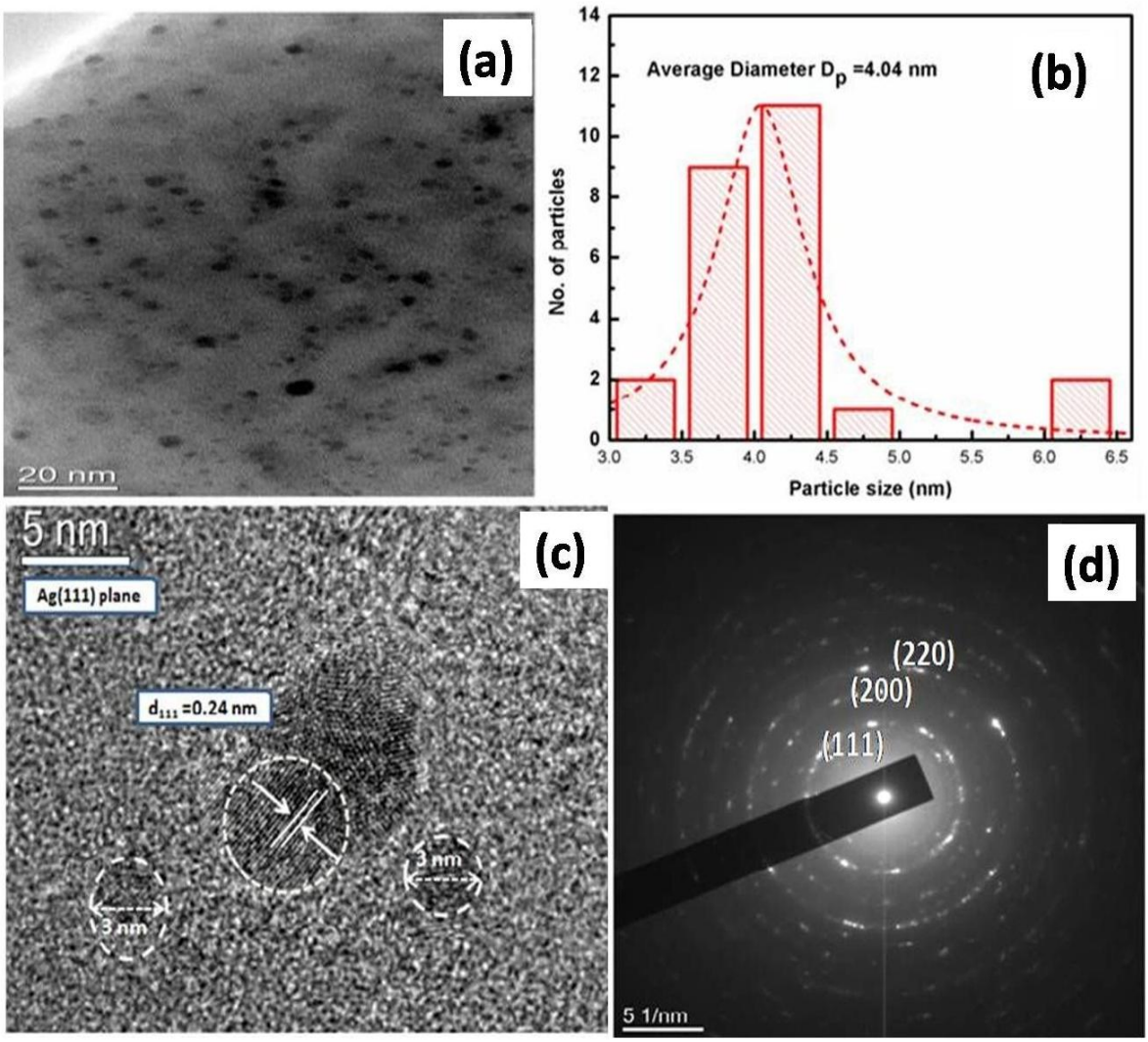


**Figure 8: FEGTEM image of silver ion exchanged glass after annealing at 550°C for 1h; (a) TEM image, (b) Average particle size by using histogram, (c) HRTEM image and (d) SAED pattern of TEM image.**

The average size of the nanoclusters estimated from the several TEM images is found to be 2.8±1, 3.3±1.2 and 4.0±1.5 nm for sample annealed at 450°C, 500°C, 550°C for 1h respectively (as shown in the histogram plot) which are in good agreement with the cluster size

calculated by using Mie theory. Analysis of high resolution TEM image and the selected area electron diffraction (SAED) pattern for sample annealed at 550°C for 1h show the polycrystalline nature of the spherical particles consisting the crystallographic plane (1 1 1) with d-spacing of 0.24 nm of $Ag^0$ clusters. These results closely match with the observations and interpretations made from the UV–Visible spectroscopy on the Ag nanoparticle growth inside the glass matrix.

The Figure 9 shows the room temperature photoluminescence spectra of $Ag^+$- $Na^+$ ion exchanged soda lime glass after annealing at various temperatures 450, 500 and 550°C for 1hr. At the excitation wavelength of 325 nm the photoluminescence spectra of thermally treated glass samples show drastic changes in PL intensity.

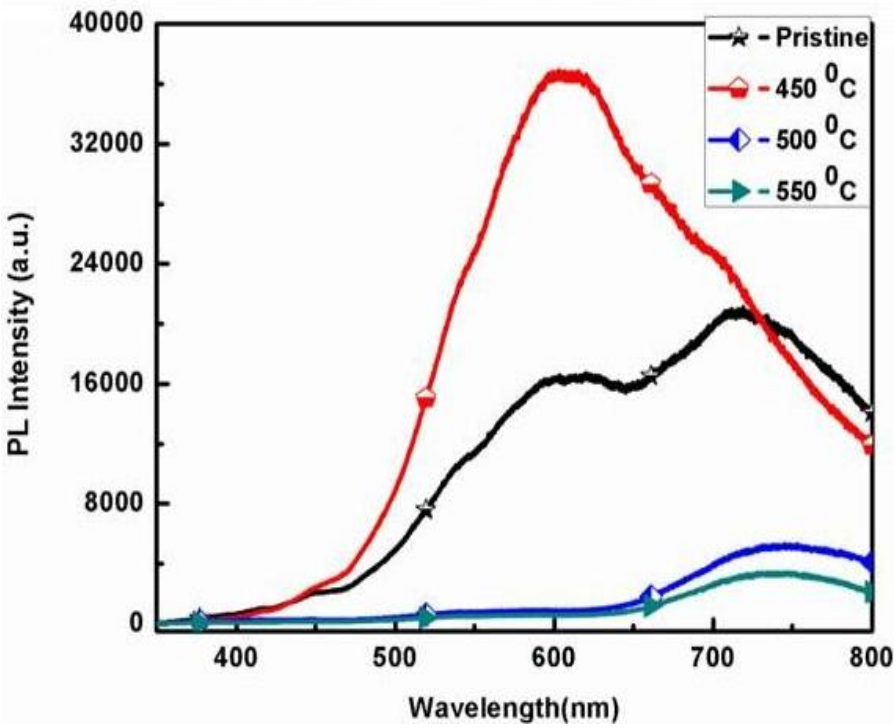


**Figure 9: PL spectra of silver ion exchanged glass samples after annealing at 450, 500, and 550°C for 1h.**

PL intensity is maximum for 450°C, but the PL intensity decreases drastically after annealing at higher temperatures (500 and 550°C) for 1 hour and is minimum at 550°C. Villegas

et al. has reported that $Ag^+$ ions are luminescent in nature in both crystalline and glassy matrices[31]. The PL emission for $Ag^0$ (neutral atoms) at any excitation wavelength has been not reported in the literature. This increase in PL intensity of the sample annealed at 450°C for 1 hr was observed which may be due to the increase of volume fraction of $Ag^+$ ions in the bulk soda lime glass matrix. The decrease in PL intensity with further ion exchange at higher temperature and/or annealing of glass samples results in reduction of $Ag^+$ ions leading to increased formation of $Ag^0$ atoms. Further increase in annealing temperature leads to the rapid growth of silver nanoparticles and that might have resulted in the quenching of PL intensity for the samples annealed at 550°C for 1h[5,32]. Gangopadhyay et al. has reported similar results for Ag nanoclusters in ion exchanged glass matrix followed by thermal annealing in vacuum[33-34]. The results shown in PL are in good agreement with the XRD patterns as the samples show amorphous nature at the annealing temperature of 450°C and 500°C.

The Figure 10 shows Rutherford backscattering spectra of pristine and thermally treated glass samples in air at 550°C for 1 h. An analyzing beam of $He^+$ ions at energy of 2 MeV, backscattered by an angle of 165°C was used during the backscattering measurements. It is observed from the Rutherford backscattering spectra that silver atoms accumulate near the surface of soda-lime glass during thermal annealing. Near-surface accumulation is due to the thermal diffusion of silver ions in the soda-lime glass matrix. This outward diffusion of silver ions relaxes the stress (which arises due to the difference in size of $Ag^+$ and $Na^+$ ions) and minimizes the total energy in the system. The ion exchange at 370°C leads to incorporation of Ag atoms into soda-lime glass matrix after substituting the Na atoms in glass matrix. These Ag atoms in ion exchanged glass exist mainly in the form of $Ag^+$ ions together with a small number of $Ag^0$ atoms[28]. The Ag-ion exchange process at higher temperature or increase in the annealing

temperature and time results in the reduction of $Ag^{+}$ ions after capturing the electrons from the glass matrix or from the impurities leading to increased formation of silver neutral atom $(Ag^{0})$[30].

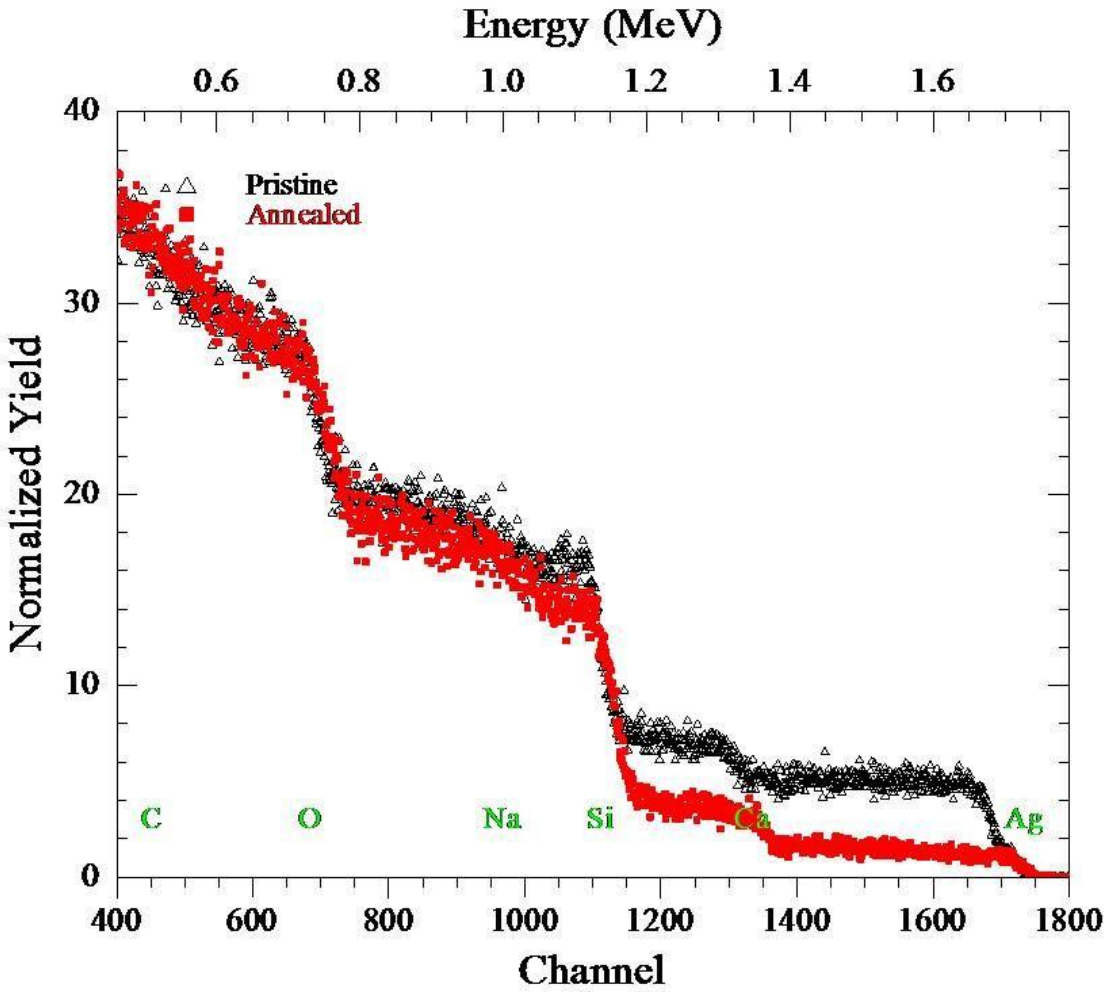


**Figure 10: RBS spectra of silver ion exchanged glass (pristine) and annealed sample at 550°C for 1h.**

Therefore the coloration of annealed samples varies with annealing temperature (light to dark red) with the increase in the size of Ag clusters. The increase in annealing temperature further increases the formation of silver $(Ag^{0})$ neutral atom. This clustering and precipitation of Ag atoms leads to the formation of Ag nanoclusters which is responsible for plasmon resonance. The silver atoms $(Ag^{0})$ are mainly bound to non-bridging oxygen (NBO) in glass matrix. During

thermal annealing Ag atoms diffuse towards the glass surface for thermal relaxation of the surface which results into the tensile stress due to the size difference after cooling[28].

The XPS core level spectra of Ag are shown in Figure 11 for the pristine sample and the sample annealed at 550°C. XPS measurements were carried out by the Perkin-Elmer PHI model using monochromatic Mg-Kα radiations (1253.6 eV), produced by 15 KV electron impact on a magnesium anode at a power level of 300 W and was used as an excitation source. The pass energy was set at 25 eV to provide a resolution of 0.5 eV. The photoelectron spectrometer work function was adjusted to get Au $4f_{7/2}$ peak at 84 eV. The binding energy of the core level photoelectron of Ag was conventionally calibrated by assuming the binding energy of the surface C 1s photoelectron to be 284.6 eV. There is no signal from pristine sample while the sample annealed at 550°C shows the spin orbit splitting of Ag-3d level.

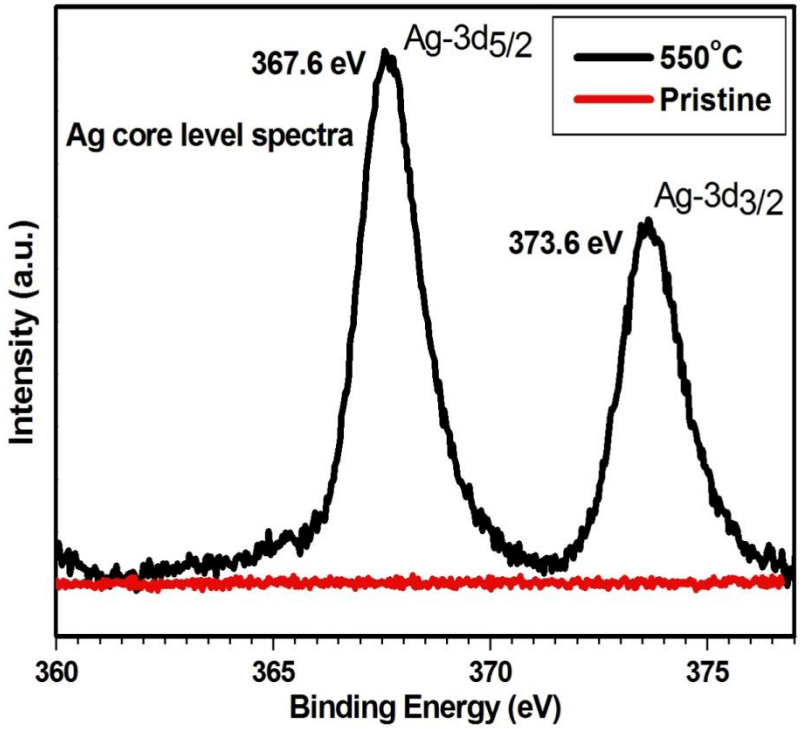


**Figure 11: XPS spectra of silver ion exchanged glass (pristine) and sample annealed at 550°C for 1h.**

The core level spectra of annealed film show Ag-$3d_{3/2}$ (~373.6 eV), Ag-$3d_{5/2}$ (~367.6 eV) positions indicating the presence of silver in metallic form in the glass matrix as the difference between two Ag peaks is 6.0 eV[35-36]. In addition the chemical shift of ~0.4 eV was observed for the Ag-3d peak towards low binding energy. This clearly indicates that the silver is also present in the form of $Ag^+$ for the formation of silver oxide ($Ag_2O$), as the required Ag-3d binding energy for this compound is in the range of 367.6 ~367.7 eV[36]. In some studies it was observed that, the chemical states of Ag associated with the Ag $3d_{5/2}$ in Ag-doped semiconducting samples exist as $Ag^0$ (metallic Ag) at 367.9 or 368.1 eV, $Ag^{2+}$ (AgO phase) at 367.0 or 367.8 eV and $Ag^+$ ($Ag_2O$ phase) at 367.6 or 367.7 eV in XPS signals respectively[36-39].

**4. Conclusions**

The synthesis of Ag nanoclusters embedded in the soda lime glass by $Na^+$-$Ag^+$ ion exchange followed by thermal annealing in air has been performed. It demonstrates that the ion exchanged Ag nanoparticles diffuse in pure soda glass matrix during annealing process. After annealing these particles are reduced to neutral silver atom ($Ag^0$) and subsequently form silver nanoparticles in the oxidizing atmosphere. The luminescence intensity of thermally exchanged samples decreases with increase in annealing temperature. Photoluminescence, XPS and RBS confirm clustering and precipitation of Ag atoms leads to the formation of Ag nanoclusters and partial formation of $Ag_2O$ phase on the surface of glass matrix with increase in the annealing temperature. TEM image shows the presence of spherical nanoparticles of average cluster size with a maximum particle size of 4 nm after annealing at 550°C for 1 hour. The clusters size calculated from Mie theory are in excellent agreement with the size measured from FEGTEM.

**Acknowledgement:**

Mr. Mohan Chandra Mathpal is thankful to CIR staff at MNNIT and the director at MNNIT for providing the characterization facility and funding support through TEQIP-II project for carrying out the research work.

**Declarations:**

The authors declare that there is no competing financial interest.

## References:

[1] S. Lal, S. Link, N. J. Halas, *Nat. Photonics*, 2007, **1**, 641−648.

[2] M. W. Knight, H. Sobhani, P. Nordlander, N. J. Halas, *Science,* 2011, **332**, 702−704.

[3] V. E. Ferry, J. N. Munday, H. A. Atwater, *Adv. Mater*., 2010, **22**, 4794−4808.

[4] A. Kumar, P. K. Vemula, P. M. Ajayan, G. John, *Nat. Mater.*, 2008, **7**, 236–241.

[5] J. C. Riboh, A. J. Haes, A. D. Mcfarland, C. R. Yonzon, R. P. V. Duyne, *J. Phys. Chem. B,* 2003, **107**, 1772–1780.

[6] D. A. Giljohann, D. S. Seferos, W. L. Daniel, M. D. Massich, P. C. Patel, C. A. Mirkin, *Angew. Chem., Int. Ed.,* 2010, **49**, 3280−3294.

[7] V. Amendola, O. M. Bakr, F. Stellacci, *Plasmonics*, 2010, **5**, 85.

[8] X. M. Zhang, J. J. Han, Q. Zhang, F. F. Qin, J. J. Xiao, *Optics Communications*, 2014, **325**, 9–14.

[9] S. Ju, V. L. Nguyen, P. R. Watekar, B. H. Kim, C. Jeong, S. Boo, C. J. Kim, W. T. Han, *J. Nanosci. Nanotechnol.* 2006, **6**, 3555-3558.

[10] K. L. Kelly, E. Coronado, L. L. Zhao, G. C. Schatz, *J. Phys. Chem. B,* 2003, **107**, 668– 677.

[11] Y. P. Sun, J. E. Riggs, K. B. Henbest, R. B. Martin, *J. Nonlinear Opt. Phys. Mater.*, 2000, **9 (4)**, 481–503.

[12] D. Ricard, P. Roussignol, C. Flytzanis, *Opt. Lett.*, 1985, **10 (10)**, 511–513.

[13] L. I. Yang, K. Becker, F. M. Smith, R. H. Magruder, J. R. F. Haglund, L. Yang, R. Dorsinville, R. R. Alfano, R. A. Zuhr, *J. Opt. Soc. Am. B, Opt. Phys.*, 1994, **11 (3)**, 457-461.

[14] T. Tokizaki, A. Nakamura, S. Kaneko, K. Uchida, S. Omi, H. Tanji, Y. Asahara, *Appl. Phys. Lett.*, 1994, **65 (8)**, 941–943.

[15] Y. Hamanaka, A. Nakamura, S. Omi, N. D. Fatti, F. Vallee, C. Flytzanis, *Appl. Phys. Lett.*, 1999, **75 (12)**, 1712–1714.

[16] N. D. Fatti, F. Vallee, Appl. Phys. B, *Lasers Opt.*, 2001, **73**, 383–390.

[17] U. Kreibig, M. Vollmer, Optical properties of metal clusters, (Springer-Verlag, Berlin), 1995.

[18] P. P. Kiran, G. De, D. N. Rao, *IEE Proc.-Circuits Devices Syst.*, 2003, **150 (6)**, 559.

[19] Y. X. Chun, L. I. Z. Hui, L. I. Weijie, X. U. J. Xian, D. Z. Wei, Q. S. Siong, *Chinese Bulletin Science*, 2008 , **53 (5)**, 695-699.

[20] R. Philip, G. R. Kumar, N. Sandhyarani, et al., *Phys. Rev. B*, 2000, **62**, 13160.

[21] G. Battaglin, P. Calvelli, E. Cattaruzza, et al., *Appl. Phys. Lett.*, 2001, **78**, 3953.

[22] K. Farah, F. Hosni, A. Mejri, B. Boizot, A. H. Hamzaoui, H. B. Ouada, *Nuclear Instruments, and Method in Physics Research B,* 2014, **323**, 36-41.

[23] Z. Dong, X. Yang, Z. Li, G. You, Y. Yan, S. Quan, *Physica B,* 2009, **404**, 2122-2125.

[24] M. C. Mathpal, P. Kumar, Balasubramaniyan. R, J. S. Chung, A. K. Tripathi, M. K. Singh, M. M. Ahmad, S. N. Pandey, A. Agarwal. *Mater. Lett*., 2014, **128**, 306- 309.

[25] F. Chen, J. Cheng, S. Dai, Y. Xu, Q. Yu, *Materials Research Bulletin,* 2013, **48**, 4667–4672.

[26] P. Manikandan, D. Manikandan, E. Manikandan, A. C. Ferdinand, *Spectrochimica Acta Part A: Molecular and Biomolecular Spectroscopy*, 2014, **124**, 203-207.

[27] M. Kumar, C. S. S. Sandeep, G. Kumar, Y. K. Mishra, R. Philip, G. B. Reddy, *Plasmonics*, 2014, **9**, 129–136.

[28] G. W. Arnold. *J Appl. Phys.*, 1975, **46**, 4466.

[29] B. Karthikeyan, *J. Appl. Phys.*, 2008, **103**, 114313

[30] C. Kittel, Introduction to Solid State Physics, 8$^{th}$ ed., Introduction to Solid State Physics, Willey Eastern, India, 2007.

[31] M. A. Villegas., *J. Sol-Gel Sci. Technol.*, 1998, **11**, 251.

[32] P. W. Wang, *Appl Surf Sci,* 1997, **120**, 291.

[33] P. Gangopadhyay, R. Kesavamoorthy, S. Bera, P. Magudapathy, K. G. M. Nair, B. K. Panigrahi, S. V. Narasimhan, *Phys. Rev. Lett.* 2005, **94**, 047403.

[34] J. Rozra, I. Saini, S. Aggarwal, A. Sharma, *Adv. Mat. Lett.*, 2013, **4(8)**, 598-604.

[35] Z. Han, J. Zhang , Y. Yu , W. Cao, *Materials Letters,* 2012, **70**, 193–196.

[36] C. D. Wagner, W. M. Riggs, L. E. Davis, J. F. Moulder, handbook of X-ray photoelectron spectroscopy. Published by Perkin-Elmer Corporation, physical electronics division.

[37] D. Brigss, M. P. Seah, in Practical Surface Analysis, Auger an X-ray Photoelectron Spectroscopy Vol. 1, 2nd ed.(Wiley, Chichester, 1990), pp. 595–634.

[38] M. A. Garcia, M. G. Heras, E. Cano, J. M. Bastidas, M. A. Villegas, E. Montero, J. Llopis, C. Sada, G. D. Marchi, G. Battaglin, P. Mazzoldi, *J. Appl. Phys.*, 2004, **96 (7)**, 3737-3741.

[39] K. Xu, J. Heo, W. J. Chung, *International Journal of Applied Glass Science*, 2011, **2(3)**, 157–161.